Study the Inhibitory Effect of some Antiviral Flavonoids against Main Protease of COVID-19 by Molecular Docking

Z. Pahlavan Yali and M.H. Fatemi

Chemometrics Laboratory, Faculty of Chemistry, University of Mazandaran, Babolsar, Iran

The potential of 39 antiviral flavonoids for inhibition of the main protease of coronavirus disease 2019 (COVID-19) was investigated using a molecular docking approach. The studied flavonoids were protease inhibitors of human immunodeficiency viruses (HIV), severe acute respiratory syndrome (SARS), hepatitis C virus (HCV), or Ebola virus. Both affinity and similarity-based molecular docking approach was applied to improve the reliability of the proposition. The estimated binding energy proposed six flavonoids for COVID-19 therapy. Then the similarity-based molecular docking arranged the candidate flavonoids respectively as *Quercetin 3-O-(2¢¢-galloyl)-R-Larabinopyranoside* from *Acer okamotoanum*, *Tomentin D* and *Tomentin A* from *Paulownia tomentosa*, *Corylifol A* and *psoralidin* from *Psoralea* and *Ladanein* from *Lamiaceae*. The values of similarity score for these phytochemicals respectively were -340, -225, -221, -213, -176, and -152 while the estimated binding energy were -9.52, -7.74, -7.67, -8.09, -8.58, and -8.02 (kcal mol^{-1}). Also, ligand map probing of native and six flavonoids was shown Phe 140, Gly 143, His 164, Glu 166, Gln 189, Thr 190, Thr 26, Cys 145, and Asn 142 amino acids of the active site of main protease of Covid-19 commonly was in the hydrogen or steric interactions with these inhibitors. This study outstanding the inhibitor effect of some antiviral non-nutrient plant compounds against the main protease of COVID-19.

Keywords: COVID-19, Molecular docking, Flavonoid, *Acer okamotoanu*, *Paulownia*, *Psoralea*, *Lamiaceae*

INTRODUCTION

The Spread of the coronavirus pandemic across the world caused a global effort to discover vaccine ines drugs [1,2]. coronavirus disease 2019 (COVID-19) is a member of the onacoronavirusrge family which are enveloped, positive-sense and single-stranded RNA (+ssRNA) viruses [3]. It is a viral infectious cause that is ter as severe acute respiratory syndrome coronavirus 2 (SARS-CoV-2) [1,2]. The rapid outbreak of COVID-19 led to observation far away from where it first appeared in Wuhan, China at the end of 2019 [1, 2].

The application of herbal drugs is one of the actual trends in antiviral therapy that appears as natural protease inhibitors [4]. This type of inhibitor prevents viruses' replication by selectively binding to their proteases and blocking proteolytic cleavage of protein precursors [5]. Flavonoids are superior antiviral drugs able to inhibit the main proteases of a variety of viral such as human immunodeficiency viruses (HIV) [6], severe acute respiratory syndrome (SARS) [7,8], or hepatitis C virus (HCV) [9].

Though, experimental determination of the inhibitory effect of all flavonoids for emergence COVID-19 therapy is costly and time-consuming, therefore, developing of theoretical approach for estimation of this effect is necessary. Molecular docking is a key approach for drug proposition which estimate the binding mode and energy of receptor protein with candidate drug [10,11]. Previously, this strategy collaborated with invitro assay analysis and was applied to investigate the protease inhibition effect of flavonoids for HCV [12], SARS [13], and Ebola [14] viruses. Accordingly, *apigenin* and *luteolin* were discovered as anti-HCV agents *via* pharmacophore search combined with a molecular docking strategy [12]. *Herbacetin*, *rhoifolin*, and, *pectolinarin* were found to efficiently block the enzymatic

---
*Corresponding author. E-mail: z.pahlavanyali@stu.umz.ac.ir

activity of SARS main protease [13]. The potential of *myricetin* as an Ebola virus VP35-double-stranded RNA of interaction inhibitor was identified through a novel fluorescence-based assay cooperated with a molecular docking approach [14]. In addition, molecular docking methodology was applied for investigating the inhibitory effect of some flavonoids against HCV [15], HIV [16], and Ebola [17-20] virus proteases.

The evaluation of the hydrogen bond potential energy has a significant impact on the drug design and development that allows the assessment of a dataset of studied organic compound screening focused on interested proteins [21-23]. The role of hydrogen bonds as the most significant noncovalent interaction in most polypeptides of proteins in biological systems is ubiquitous the function of biological molecules is to a large degree determined by H-bonds; in an aqueous environment, where H-bonding interactions are responsible for many of the properties and is an extremely important aspect in the structural organic chemistry of biomaterials such as proteins and DNA [23-25]. The importance, necessity, and potency of computational approaches to investigated and hydrogen bonds can be seen in some studies as [25-30]. The molecular docking strategy also is one of the best techniqes can to index the involved medicinal fragments and amino acids residues of the target proteins in vindicator of inhibitory effect and their probable mechanism [22,31,32]. The evaluation of the hydrogen bond potential energy has a significant impact in the drug design and development that allows the assessment of a dataset of studied organic compound screening focused on interested proteins [31,32]. The strong inhibitor binding which are reflected according frequency of hydrogen bonds the most of the inhibitors were found to involve in hydrophobic interactions with the receptors. The molecular docking results shown in figures confirmed that the hydrogen interactions or bonding with the target have pivotal contributions in binding structures and free energies while van der Waals and Pi-interactions contributed to the stabilization of the binding structures [22].

This work attempt to assist the inhibitory effect of 39 antiviral flavonoids for emergence COVID-19 therapy. A molecular docking approach was applied for the estimation of blocking ability against the main protease of COVID-19. The collaboration of affinity and similarity-based molecular docking improve the reliability of recommendable herbal inhibitor.

MOLECULAR DOCKING STUDY

The structures of 39 studied flavonoids were drawn and optimized by the semi-empirical AM1 method using the Hyperchem program (version 7) [33]. Antiviral therapeutic applications and sources of these natural compounds was mentioned in Table 1. The antiviral therapy of candidate flavonoids appeared for SARS, HIV, HCV, and Ebola. In the next step, the crystallography structure of protease of COVID-19 (6LU7) was taken from a protein data bank (PDB).

Firstly, the affinity-based molecular docking approach was done using MGLTools (version 1.5.6) [34] software. A grid box with $60 \times 60 \times 60$ points was defined in the inhibitory site and the Lamarckian search algorithm was used with default values of genetic algorithm parameters. The predicted binding energy of flavonoids compared with the co-crystalized inhibitor of protease for COVID-19 (N3) [35-37]. The chemical name of the co-crystalized ligand N3 is n-[(5-methylisoxazol-3-yl)carbonyl]alanyl-l-valyl-n~1~-((1r,2z)-4-(benzyloxy)-4-oxo-1-{[(3r)-2-oxopyrrolidin-3-yl]methyl} Sbut-2-enyl)-l-leucinamide [38].

In the last step, the similarity based molecular docking approach was performed using Molegro Virtual Docker (MVD) with application of a search algorithm MolDcok SE (simplex evolution) [35]. The search space with radius of 27 Å was defined in the inhibitory site of COVID-19 for a similarity screening against template co-crystalized N3. Template are implemented as scoring function rewarding poses similar to specified pattern [35-37]. A template is considered as a collection of template groups which represent the chemical features and contains a number of centers. Steric group matches all atoms and was used for shape matching without taking any chemical groups into account. The matching of an atom with defined groups rewarded using a Gaussian formula which weight of template groups (ω) in this equation set up by a strength factor. The Gaussian formula for each center was calculated as follow:

$$e = \omega * \exp(-d^2/r_0^{\,2})$$

Table 1. Flavonoids Name and their Estimated Binding Energy with Main Protease of COVID-19

No.	Flavonoids Name	Treatment	Source	Binding energy (Kcal mol^{-1})
1	Quercetin	HCV [27]	*Embelia ribes* [27], *Pichia pastoris* [28]	-7.22
2	Apigenin	SARS [28] HCV [27,29], HIV [30]	*Embelia ribes* [27], *Pistacia chinensis* [29], *Galangin, Fisetin, Irans-chalcone* [30]	-7.05
3	Rutin	HCV [31]	*Prunus domestica* [31]	-7.00
4	Isoliquiritigenin	HCV [32]	*Glycyrrhizae radix* [32]	-6.63
5	Glycycoumarin	HCV [32]	*Glycyrrhizae radix* [32]	-7.34
6	Naringenin	HCV [33, 34]	*Grapefruit* [33]	-6.12
7	Pedalitin	HCV [35]	*Pterogyne nitens* [35]	-7.07
8	Sorbifolin	HCV [35]	*Pterogyne nitens* [38]	-7.01
9	Diosmetin (4'-methoxy luteolin)	HCV[36]	*Pistacia chinensis* [36]	-6.68
10	Eriodictyol 7-O-(6″-caffeoyl)-β-D-glucopyranoside	HCV [37]	*lsholtzia bodinieri* [37]	-7.54
11	Eriodictyol [29]	HCV [29]	*Pistacia chinensis* [29]	-6.63
12	Diosmetin	HCV [29]	*Pistacia chinensis* [29]	-7.24
13	Ladanein	HCV [9]	*Marrubium peregrinum L* [9]	-8.02
14	Apigenin 7-O-beta-D-(4'-caffeoyl)glucuronide (1)	HIV [38]		-6.8
15	Acacetin	HIV [30]	Galangin, Fisetin, Irans-chalcone [30]	-7.01
16	Chrysin	HIV [30,39]	*Galangin, Fisetin, Irans-chalcone* [30], *Chrysanthemum morifolium* [39]	-7.00
17	2-Methoxy-3-methyl-4,6-dihydroxy-5-(30-hydroxy)cinnamoylbenzaldehyde	HIV [40]	*Genus Desmos* [40]	-5.57
18	Quercetin 3-*O*-(2¢¢-galloyl)-R-Larabinopyranoside	HIV [6]	*Acer okamotoanum* [6]	-6.82
19	Quercetin 3-*O*-(2¢¢-galloyl)-R-Larabinopyranoside	HIV [6]	*Acer okamotoanum* [6]	-9.52
20	2-Methoxy-3-methyl-4,6-dihydroxy-5-(30-hydroxy)cinnamoylbenzaldehyde	HIV [40]	*Genus Desmos* [40]	-5.57
21	Luteolin	HIV [41]	_	-7.02
22	Myricetin	Ebola [14], SARS [42]	*l.morisianum* [14], *Chromadex* [42]	-7.26
23	Epigallocatechin gallate	SARS [28], HCV [43,44]	*Pichia pastoris* [28]	-6.87
24	Gallocatechin gallate	SARS [28]	*Pichia pastoris* [28]	-7.66
25	Scutellarein	SARS [42]	*Scutettaria baicalensis* [42]	-6.31
26	Herbacetin	SARS [13]	_	-6.72
27	Rhoifolin	SARS [13]	_	-6.59
28	Pectolinarin	SARS [13]	_	-6.58
29	Bavachinin	SARS [7]	*Psoralea* [7]	-7.41
30	Neobavaisoflavon	SARS [7]	*Psoralea* [7]	-7.63
31	Isobavachalcone	SARS [7]	*Psoralea* [7]	-5.89
32	40-O-methylbavachalcone	SARS [7]	*Psoralea* [7]	-6.90
33	Psoralidin	SARS [7]	*Psoralea* [7]	-8.58
34	Corylifol A	SARS [7]	*Psoralea* [7]	-8.09
35	Tomentin A	SARS [8]	*Paulownia tomentosa* [8]	-7.67
36	Tomentin B	SARS [8]	*Paulownia tomentosa* [8]	-7.63
37	Tomentin C	SARS [8]	*Paulownia tomentosa* [8]	-7.29
38	Tomentin D	SARS [8]	*Paulownia tomentosa* [8]	-7.74
39	Tomentin E	SARS [8]	*Paulownia tomentosa* [8]	-4.89

In the above equation, d is the distance from the position of the atom to the center of the group and r_0 is a distance parameter specify a characteristic distance for the template group. The strength factor is multiplied onto all interaction energies for the sidechains contains atomic pairwise steric interactions, hydrogen bonding and electrostatic interactions. If a sidechain is very flexible, its strength set to zero in order to turn all the sidechain interactions off during the similarity screening. Notice that the strength factor does not change the interactions of the backbone atom. Also, it should be mentioned, for each atom in the template ligand, score contributions from all centers in the all matching groups are taken into account. Accordingly, a single atom may contribute to several centers in the several groups and an atom is not restricted to the closest matching center or a single group. Template groups of co-crystalized ligand was visualizaed in Fig. 1.

RESULT AND DISCUSSION

The result of affinity-based molecular docking for 39 proposed flavonoids was shown in Table 1. In this table was seen that the binding energy was varied from -9.52 (kcal mol^{-1}) for *Quercetin 3-O-(2¢¢-galloyl)-R-Larabinopyranoside* from *Acer okamotoanum* to -4.89 (kcal mol^{-1}) for *Tomentin E* from *Paulownia tomentosa* plant. It can be seen, six flavonoids contain *Quercetin 3-O-(2¢¢-galloyl)-R-Larabinopyranoside* [6], *Psoralidin* [7], *Corylifol A* [7], *Ladanein* [9], *Tomentin D* [8] and *Tomentin A* [8] proposed for COVID-19 therapy. The estimated binding energy respectively was -9.52, -8.58, -8.09, -8.07, -7.74, and 7.67 (kcal mol^{-1}). This value for co-crystalized N3 was equal to -7.67 (kcal mol^{-1}). Accordingly, these six flavonoids with predicted binding energy greater than this value for co-crystalized inhibitor N3 was recommended for inhibition of the main protease of COVID-19.

Then, similarity-based molecular docking was done for ranking the candidate flavonoids. Hydrogen donor and acceptor, negative and positive charge as well as ring groups features were considered with a co-strength 1. Also, in this screening steric criteria were involved with strength 0.5 being considered for the estimation of similarity. The optimal conformation of these phytochemicals with the most MolDock scores was selected with the aim of estimating the similarity. Accordingly, candidate flavonoids were arranged respectively as *Quercetin 3-O-(2¢¢-galloyl)-R-Larabinopyranoside*, *Tomentin D*, *Tomentin A*, *Corylifol A*, *psoralidin*, and *Ladanein*. The values of similarity score for these flavonoids respectively were -340, -225, -221, -213, -176, and -152 (kcal mol^{-1}). The position of co-crystalized ligand N3 and proposed flavonoids bind to the main protease of COVID-19 was shown in Fig. 2.
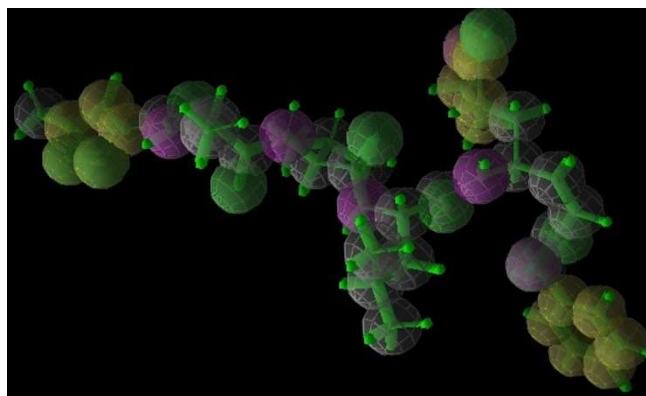

Fig. 1. Visualization of template groups of native inhibitor N3 (green); hydrogen donor (purple), hydrogen acceptor (green), ring groups (yellow) and steric criteria (gray).
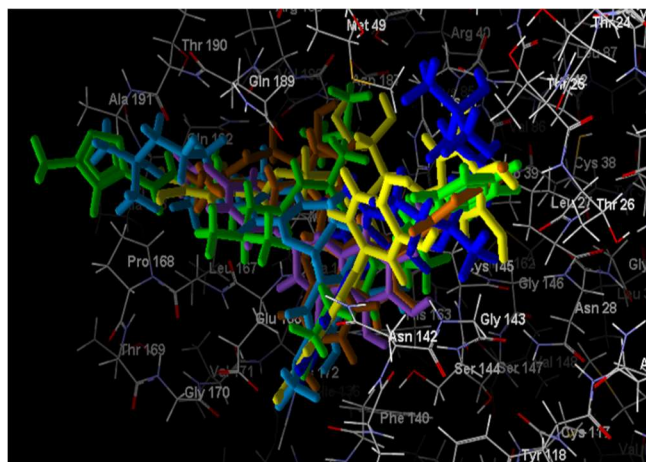

Fig. 2. Position of N3 (green) and six proposed antiviral flavonoids a) *Quercetin 3-O-(2¢¢-galloyl)-R-Larabinopyranoside* from *Acer okamotoanum* (yellow), b) *Tomentin D* and *Tomentin A* from *Paulownia tomentosa* (light and dark blue) c) *Corylifol A* and *psoralidin* from *Psoralea* (light and dark brown) and d) *Ladanein* from *Lamiaceae* (purple) in the active site of main protease of Covid-19.
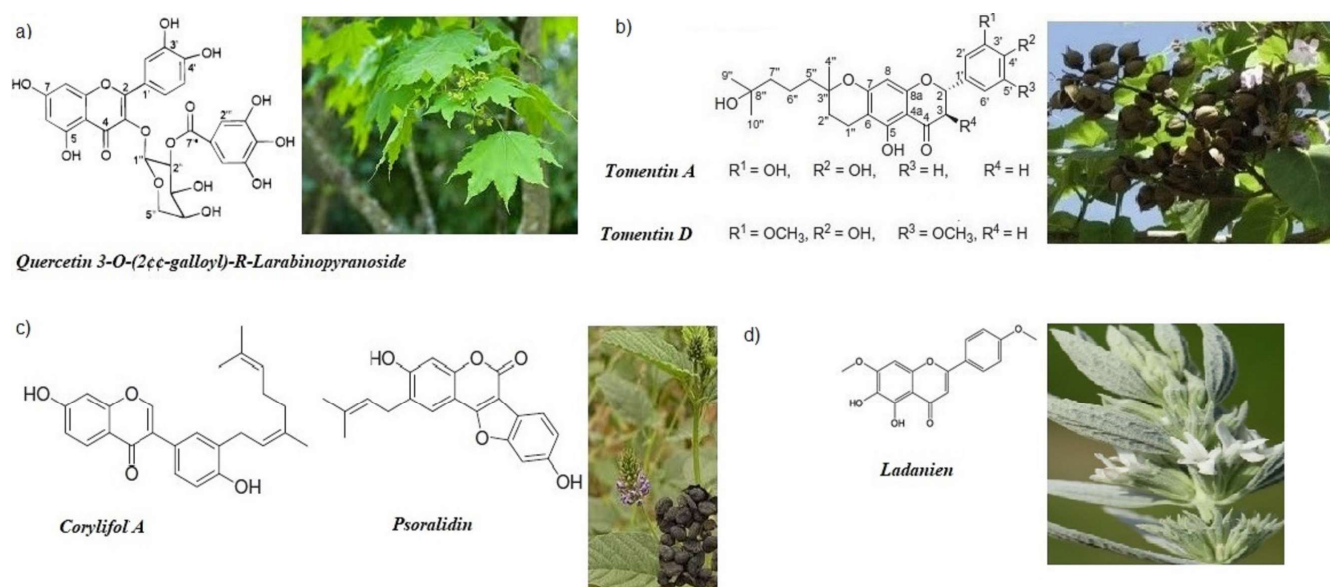
Fig. 3. Chemical structure of proposed inhibitor flavonoids for main protease of Covid-19 and their natural sources plants; a) *Acer okamotoanum*, b) *Paulownia tomentosa*, c) *Psoralea* and d) *Lamiaceae*.
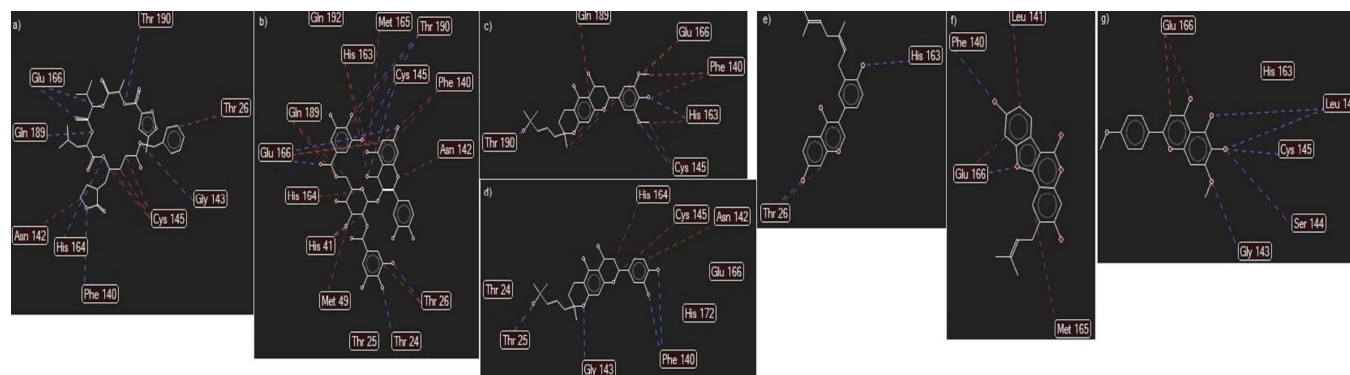

Fig. 4. Hydrogen bonds and steric interactions of N3 and six proposed flavonoids in active site of main protease of Covid-19.

Quercetin 3-O-(2¢¢-galloyl)-R-Larabinopyranoside is a glycoside gallate ester flavonol from leaves of *Acer okamotoanum* that its inhibitory activity was integrated against HIV [6]. *Tomentin D* and *Tomentin A* are the geranylated flavonoids from the fruits of *Paulownia tomentosa* that displa SARS-CoV papain-like protease inhibition [8]. *Corylifol A* and *psoralidin* are the phenolic phytochemical from the seeds of P*soralea corylifolia* (*Psoralea*) that display an inhibition for SARS-CoV papain-like protease [7]. *Ladanein* is a phenolic compound from

flowered aerial parts of *Marrubium peregrinum L* (*Lamiaceae*) with a potent against HCV [9]. The chemical structure and pictures of *Acer okamotoanum*, *Paulownia tomentosa*, *Psoralea,* and *Lamiaceae* plants that source of six proposed flavonoids respectively was shown in Fig. 3.

Furthermore, ligand map probing of native and six phytochemical inhibitors respectively was shown in Figs. 4a, b, c, d, e, f and g that it can be seen, hydrogen bonds and steric interaction determine this interlock for both native and suggested flavonoids. The hydrogen interactions with Phe

140, Gly 143, His 164, Glu 166, Gln 189, and Thr 190 amino acids and steric interaction with Thr 26, Cys 145, and Asn 142 amino acids were seen for native inhibitor. The hydrogen interactions *Quercetin 3-O-(2¢¢-galloyl)-R-Larabinopyranoside* with Cys 145, Glu 166, and Thr 190 amino acids and steric interaction with Thr 26, Phe 140, Asn 142, Cys 145, His 164, Glu 166, Thr 190, and Gln 189 amino acids were in the active site of main protease of Covid-19. The hydrogen interactions *Tomentin D* with Cys 145, and Thr 190 amino acids and steric interaction with Cys 145 Phe 140, Glu 166, and Gln 189 while *Tomentin A* was in the steric interaction with Phe 140, Gly 143, Cys 145, and His 164. The hydrogen and steric interactions of *Corylifol A* were with Thr 26 while *psoralidin* was in the hydrogen interaction with Phe 140 and Glu 166 and also a steric interaction with Glu 166. Also, *Ladanein* flavonoids were hydrogen interactions with Gly 143 and Cys 145 and steric interactions with Glu 166.

In the other perspective it was seen that the hydrogen and steric interactions with Thr 26 was observed in Fig. 4e with *Corylifol A* as well as steric interactions was seen in Fig. 4b between the *Quercetin 3-O-(2¢¢-galloyl)-R-Larabinopyranoside* flavonoids and Asn 142. The both hydrogen bonds and steric interactions of *Quercetin 3-O-(2¢¢-galloyl)-R-Larabinopyranoside* and *Tomentin D* respectively were seen with Thr 190 and Gln 189 amino acid of active site in Figs. 4b and d. Also, the steric interactions were appeared with *Quercetin 3-O-(2¢¢-galloyl)-R-Larabinopyranoside* and *Tomentin A* flavonoids for His 164 while the hydrogen interactions with Gly 143 amino acid of active site of main protease of Covid-19 was seen with *Tomentin A* and *Ladanein* respectively in Figs. 4b and d) and Figs. 4d and g. The steric interactions were seen between Glu 166 and *psoralidin* and *Ladanein* respectively in Figs. 4f and g. The hydrogen interactions of *Tomentin A and psoralidin*, and steric interactions of *Quercetin 3-O-(2¢¢-galloyl)-R-Larabinopyranoside* and *Tomentin D* with Phe 140 were seen in Figs. 4b, c, d and f. Also, the hydrogen interactions of *Quercetin 3-O-(2¢¢-galloyl)-R-Larabinopyranoside* and *psoralidin* as well as steric interactions of *Quercetin 3-O-(2¢¢-galloyl)-R-Larabinopyranoside, psoralidin*, *Tomentin D* and *Ladanein* with Glu 166 was seen in Figs. 4b, c, f and g. In addition, Cys 145 was the hydrogen interactions with the *Quercetin 3-O-(2¢¢-galloyl)-R-Larabinopyranoside, Tomentin D*, and *Tomentin A* as well as steric interactions

with *Quercetin 3-O-(2¢¢-galloyl)-R-Larabinopyranoside, Tomentin D,* and *Ladanein* (Figs. 4b, c, d and g). Overall, the exploration of hydrogen interactions of candidate inhibitors in conformational space surrounding amino acids at the active binding site can show the frequency conflict of Phe 140, Gly 143, His 164, Glu 166, Gln 189, Thr 190, Cys 145, and Asn 142 as inhibition site. Regardless, this paper supplied precious insight into the non-nutrient antiviral plant chemicals that is worth considering for the therapeutic aim of COVID-19.

CONCLUSION

The inhibitor activity of 39 antiviral flavonoids was investigated for main protease of COVID-19 using molecular docking approach. First molecular docking candidate six flavonoids for COVID-19 therapy. Then, the second molecular docking ranked the proposed flavonoids with a similarity screening with co-crystalized N3 inhibitor. *Quercetin 3-O-(2¢¢-galloyl)-R-Larabinopyranoside*, *Tomentin D*, *Tomentin A*, *Corylifol A*, *psoralidin* and *Ladanein* flavonoids respectively candidate for COVID-19 therapy. The values of similarity score for these compounds was -340, -225, -221, -213, -176 and -152 (kcal mol^{-1}) while the predicted binding energy was -9.52, -7.74, -7.67, -8.09, -8.58 and -8.02 (kcal mol^{-1}). The ligand map probing of native and proposed flavonoids was shown that the hydrogen interactions *Quercetin 3-O-(2¢¢-galloyl)-R-Larabinopyranoside* with Cys 145, Glu 166, and Thr 190 and steric interaction with Thr 26, Phe 140, Asn 142, Cys 145, His 164, Glu 166, Thr 190, and Gln 189. *Tomentin D* was in the hydrogen interactions with Cys 145 and Thr 190 and steric interaction with Cys 145 Phe 140, Glu 166, Gln 189 and *Tomentin A* was in the steric interaction with Phe 140, Gly 143, Cys 145, His 164. *Corylifol A* was in the hydrogen and steric interactions with Thr 26 and *psoralidin* was in hydrogen interaction with Phe 140 and Glu 166 as well as a steric interaction with Glu 166. Finally, *Ladanein* was hydrogen interactions with Gly 143 and Cys 145 and also a steric interaction with Glu 166. This study prominent the inhibitor activity of some HIV, SARS, and HCV natural inhibitor for COVID-19 therapy.

List of Abbreviations

COVID-19	Coronavirus disease 2019
+ssRNA	Positive-sense and single-stranded RNA
SARS	Severe acute respiratory syndrome
SARS-CoV-2	Severe acute respiratory syndrome-coronavirus-2
HIV	Human immunodeficiency viruses
HCV	Hepatitis C virus
PDB	Protein data bank
MVD	Molegro Virtual Docker

REFERENCES

[1] S.P. Adhikari, S. Meng, Y.-J. Wu, Y.-P. Mao, R.-X. Ye, I Infect. Dis. Poverty. 9 (2020) 1.

[2] C.-C. Lai, T.-P. Shih, W.-C. Ko, H.-J. Tang, P.-R. Hsueh, Int. J. Antimicrob. Agents. 55 (2020) 105924.

[3] M. Pal, G. Berhanu, C.H. Desalegn, V. Kandi, S An Update. Cureus. 12 (2020) 7423.

[4] H. Zakaryan, E. Arabyan, A. Oo, K. Zandi, Arch. Virol. 162 (2017) 2539.

[5] A. Patick, K. Potts, Clin. Microbiol. Rev. 11 (1998). 614.

[6] H.J. Kim, E.-R. Woo, C.-G. Shin, H. Park, J. Nat. Prod. 61 (1998) 145.

[7] D.W. Kim, K.H. Seo, M.J. Curtis-Long, K.Y. Oh, J.-W. Oh, J. Enzyme Inhib. Med. Chem. 29 (2014) 59.

[8] J.K. Choa, M.J. Curtis-Longc, K.H. Lee, D.W. Kim, H.W. Ryu, Med. Chem. 21 (2013) 3051.

[9] S. Haid, A. Novodomská, J. Gentzsch, C. Grethe, S. Geuenich, Gastroenterology 143 (2012) 213.

[10] P.H.M. Torres, A.C.R. Sodero, P. Jofily, F.P. Silva-Jr, Int. J. Mol. Sci. 20 (2019) 4574.

[11] S. Kotha, Y.B. Adimulam, K. Kumar, Int. J. Comput. Appl. 975 (2015) 8887.

[12] M.-M. Liu, L. Zhou, P.-L. He, Y.-N. Zhang, J.-Y. Zhou, Eur. J. Med. Chem. 52 (2012) 33.

[13] S. Jo, S. Kim, D. HShin, M.-S. Kim, J. Enzyme Inhib. Med. Chem. 35 (2020) 145.

[14] G.L. Daino, A. Frau, C. Sanna, D. Rigano, S. Distinto, Biochemistry 57 (2018) 6367.

[15] F.B. Akher, A. Farrokhzadeh, P. Ramharack, L. Shunmugam, F.R.V. Heerden, Med. Hypotheses. 132 (2019) 109359.

[16] R.H.A. Santosa, M.M.C. Ferreira, F.A. Molfetta, A.J. Camargo, K.M. Honório, J. Med. Chem. 38 (2003) 929.

[17] K. Dhama, K. Karthik, R. Khandia, S. Chakraborty, A. Munjal, Front. Immunol. 9 (2018) 1803.

[18] V. Veljkovic, P.M. Loiseau, B. Figadere, S. Glisic, N. Veljkovic, F1000Researc. 1 (2015) 4.

[19] U. Raj, P.K. Varadwaj, Interdisc Sci. 8 (2016) 132.

[20] M.A.F. Nasution, A.H. Alkaff, U.S.F. Tambunan, AIP Conference Proceedings 2023 (2018) 020055-1.

[21] P.C. Reboredo, J.L. Blanco, N.R. Fernández, F. Cedrón, F.J. Novoa, A. Carballal, V. Maojo, A. Pazos, C.F. Lozano, CSBJ. 19 (2021) 4538.

[22] D.E. Arthur, A. Uzairu, J. King Saud. Univ. Sci. 31 (2019) 1151.

[23] E.D. Głowacki, M.I. Vladu, S. Bauer, N.S. Sariciftci, J. Mater. Chem. B 1 (2013) 3742.

[24] G. Desiraju, T. Steiner, Oxford Academic Press (1999) 343.

[25] K. Wojtkowiak, A. Jezierska, J. Pharm. 16 (2023) 479.

[26] H. Roohi, B. Mackiabadi, BCSJ. 80 (2007) 1914.

[27] M. Zakarianezhad, S.M. Habibi-Khorassani, M.T. Maghsoodlou, B. Makiabadi, H. Ghasempour, IJST. 28 (2012) 251.

[28] S. Bagheri, H. R.Masoodi, M. Mohammadi, M. Zakarianezhad, B. Makiabadi, Chem. Phys. Lett. 572 (2013) 26.

[29] B. Makiabadi, M. Zakarianejad, S. Bagheri, H.R. Masoodi, R.S. Aghaie, Int. J. Quantum Chem. 113 (2013) 2361.

[30] B. Makiabadi, H. Kian, Monatsh. Chem. 146 (2015) 69.

[31] G. Bitencourt-Ferreira, M. Veit-Acosta, W.F.A. Jr. 2053 (2019) 93.

[32] M.A. Williams, J.E. Ladbury, Wiley (2003) 137.

[33] HyperChem, H., Release 7 for *windows*. HyperCube, Ed, 2002.

[34] http://mgltools.scripps.edu.

[35] R. Thomsen, M.H. Christensen, J. Med. Chem. 49 (2006) 3315.

[36] P. Chauhan, M. Shakya, Bioinformation 4 (2009) 223.

[37] N.B. Muppalaneni, A.A. Rao, Bioinformation 8 (2012) 980.

[38] Z. Jin, Z. Jin, X. Du, Y. Xu, Y. Deng, Nature 582 (2020) 289.